The Blimp1–Bcl6 axis is critical to regulate osteoclast differentiation and bone homeostasis

Yoshiteru Miyauchi,[1] Ken Ninomiya,[1] Hiroya Miyamoto,[1]
Akemi Sakamoto,[6] Ryotaro Iwasaki,[3] Hiroko Hoshi,[1] Kana Miyamoto,[1]
Wu Hao,[1] Shigeyuki Yoshida,[3] Hideo Morioka,[1] Kazuhiro Chiba,[1]
Shigeaki Kato,[7] Takeshi Tokuhisa,[6] Mitinori Saitou,[8] Yoshiaki Toyama,[1]
Toshio Suda,[4] and Takeshi Miyamoto[1,2,5,9]

[1]Department of Orthopedic Surgery, [2]Department of Integrated Bone Metabolism and Immunology, [3]Department of Dentistry and Oral Surgery, [4]Department of Cell Differentiation, The Sakaguchi Laboratory of Developmental Biology, [5]Keio Kanrinmaru Project, Keio University School of Medicine, Shinjuku-ku, Tokyo 160-8582, Japan
[6]Department of Developmental Genetics, Graduate School of Medicine, Chiba University, Chiba 260-8670, Japan
[7]Institute of Molecular and Cellular Bioscience, University of Tokyo, Bunkyo-ku, Tokyo 113-0032, Japan
[8]Department of Anatomy and Cell Biology, Graduate School of Medicine, Kyoto University, Yoshida-Konoe-cho, Sakyo-ku, Kyoto 606-8501, Japan
[9]Precursory Research for Embryonic Science and Technology, Japan Science and Technology Agency, Kawaguchi, Saitama 332-0012, Japan

Controlling osteoclastogenesis is critical to maintain physiological bone homeostasis and prevent skeletal disorders. Although signaling activating nuclear factor of activated T cells 1 (NFATc1), a transcription factor essential for osteoclastogenesis, has been intensively investigated, factors antagonistic to NFATc1 in osteoclasts have not been characterized. Here, we describe a novel pathway that maintains bone homeostasis via two transcriptional repressors, B cell lymphoma 6 (Bcl6) and B lymphocyte–induced maturation protein–1 (Blimp1). We show that Bcl6 directly targets 'osteoclastic' molecules such as NFATc1, cathepsin K, and dendritic cell–specific transmembrane protein (DC-STAMP), all of which are targets of NFATc1. Bcl6-overexpression inhibited osteoclastogenesis in vitro, whereas Bcl6-deficient mice showed accelerated osteoclast differentiation and severe osteoporosis. We report that Bcl6 is a direct target of Blimp1 and that mice lacking Blimp1 in osteoclasts exhibit osteopetrosis caused by impaired osteoclastogenesis resulting from Bcl6 up-regulation. Indeed, mice doubly mutant in Blimp1 and Bcl6 in osteoclasts exhibited decreased bone mass with increased osteoclastogenesis relative to osteoclast–specific Blimp1–deficient mice. These results reveal a Blimp1–Bcl6–osteoclastic molecule axis, which critically regulates bone homeostasis by controlling osteoclastogenesis and may provide a molecular basis for novel therapeutic strategies.

CORRESPONDENCE
Takeshi Miyamoto:
miyamoto@sc.itc.keio.ac.jp

Abbreviations used: Bcl6, B cell lymphoma 6; Blimp1, B lymphocyte–induced maturation protein 1; BMM, BM macrophage; ChIP, chromatin immunoprecipitation; cKO, conditional KO; Ctsk, cathepsin K; DC-STAMP, DC-specific transmembrane protein; DKO, double KO; NFATc1, nuclear factor of activated T cells 1; PGC, primordial germ cell; RANKL, receptor activator of NF-κB ligand; TRAP, tartrate-resistant acid phosphatase.

Osteoclasts are responsible for bone resorption, and thereby play an essential role in maintaining bone volume and homeostasis (Karsenty and Wagner, 2002). Dysregulation of osteoclast differentiation or function disrupts maintenance of bone homeostasis, which in turn leads to pathogenic conditions such as osteoporosis, rheumatoid arthritis, lytic bone metastases, or Paget's bone disease (Rodan and Martin, 2000). Thus, osteoclasts could potentially be targeted therapeutically to treat skeletal disorders. Osteoclasts originate from BM–derived monocyte/macrophage precursor cells of hematopoietic origin and are differentiated by signaling through the receptor activator of NF-κB ligand (RANKL; Kong et al., 1999). RANKL induces osteoclast differentiation by activating the nuclear factor of activated T cells 1 (NFATc1),

a transcription factor required for osteoclastogenesis (Takayanagi et al., 2002; Koga et al., 2004; Sato et al., 2006; Shinohara et al., 2008). Activated NFATc1 induces expression of "osteoclastic" molecules essential for osteoclast differentiation and function, such as DC-specific transmembrane protein (DC-STAMP) to facilitate cell–cell fusion, cathepsin K (Ctsk) to promote bone matrix proteolysis, and NFATc1 to drive differentiation (Yagi et al., 2005; Li et al., 2006). Thus, signaling pathways mediated by positive regulators of NFATc1 in osteoclastogenesis have been intensively studied, whereas factors negatively modulating osteoclastogenesis are largely unknown.

B lymphocyte–induced maturation protein 1 (Blimp1) has been investigated in numerous cell types (John and Garrett-Sinha, 2009) and is reportedly essential for specification and maintenance of primordial germ cells (PGCs) through silencing of somatic programs (Ohinata et al., 2005). B cell lymphoma 6 (Bcl6) was originally identified as a protooncogene because its chromosomal translocation and constitutive expression promotes lymphomagenesis (Ohno, 2006). $Bcl6^{-/-}$ mice show impaired germinal center formation (Fukuda et al., 1997). The roles of Blimp1 and Bcl6 have also been investigated in B cell and plasma cell development (Turner et al., 1994; Fukuda et al., 1997), as well as in T cells (Dent et al., 1998; Kusam et al., 2003; Ichii et al., 2004; Kallies et al., 2006; Martins et al., 2006; Cimmino et al., 2008). However, the roles of Blimp1 and Bcl6, both of which are transcriptional repressors, have not previously been characterized in osteoclastogenesis or skeletal disorders, although mutations in Bcl6-associated molecules are reportedly seen in skeletal pathologies such as malformation of fingers and clavicles (Ng et al., 2004). Recently, it was reported that inhibiting NFATc1 using the NFATc1 inhibitor FK506 actually resulted in reduced bone mass caused by inhibition of bone formation that was more potent than inhibition of osteoclastogenesis (Koga et al., 2005). Therefore, additional regulators of osteoclast differentiation have been sought as factors that could potentially increase bone mass.

In this study, we identify two transcriptional repressors controlling osteoclastogenesis, Bcl6 and Blimp1. We show that Bcl6 negatively regulates expression of osteoclastic genes, i.e., *NFATc1*, *DC-STAMP*, and *Ctsk*, which are all NFATc1 targets. We found that Bcl6 is recruited to promoters of these genes, and that Bcl6 inhibits osteoclastogenesis. We also report that Blimp1 binds to the *Bcl6* promoter, likely suppressing its expression. Bcl6-deficient mice exhibited decreased bone mass with increased osteoclastogenesis, whereas osteoclast–specific Blimp1 conditional KO (cKO) mice showed impaired osteoclast differentiation and increased bone mass, likely resulting from Bcl6 dysregulation. Overall, our data demonstrate that an axis of transcriptional repressors is crucial to regulate osteoclastogenesis and bone homeostasis.

RESULTS
Bcl6 is a negative regulator of osteoclastogenesis
RANKL stimulates osteoclastogenesis by activating NFATc1 (Takayanagi et al., 2002; Koga et al., 2004; Sato et al., 2006;

Shinohara et al., 2008). To identify genes potentially suppressed after RANKL stimulation of osteoclast precursor cells (BM macrophages [BMMs]), we undertook comparative microarray screens of BMMs treated with or without RANKL and found that expression of the transcriptional repressor *Bcl6* was down-regulated by RANKL (Fig. 1 A). *Bcl6* down-regulation by RANKL was confirmed by real-time RT-PCR, immunofluorescence, and immunoblot analysis (Fig. S1 and Fig. 1 B). Immunofluorescence analysis showed that Bcl6 was detected in the nuclei of M-CSF–dependent macrophages, but not in nuclei of multinuclear osteoclasts induced by RANKL (Fig. 1 B). Interestingly, chromatin immunoprecipitation (ChIP) assays showed that, in the absence of RANKL, Bcl6 was recruited to the *NFATc1* P1 promoter, a region critical for regulating *NFATc1* expression in osteoclasts, and was dismissed from the promoter after RANKL treatment. In contrast, NFATc1, an essential positive regulator of osteoclastogenesis, was absent from the *NFATc1* P1 promoter in the absence of RANKL, but recruited after RANKL stimulation (Fig. 1 C). These results suggest a potential role of Bcl6 in inhibiting osteoclastogenesis. Bcl6 overexpression also potently inhibited osteoclast differentiation in vitro (Fig. 1 D), suggesting that Bcl6 negatively regulates osteoclast differentiation and that its down-regulation after RANKL stimulation is critical to induce osteoclastogenesis.

Bcl6 deficiency facilitates osteoclast formation
To characterize the physiological roles of Bcl6 in osteoclastogenesis, we analyzed Bcl6-deficient ($Bcl6^{-/-}$) mice. $Bcl6^{-/-}$ mice exhibited lower bone mass as detected by microradiographical and dual-energy x-ray absorptiometry analysis compared with heterozygous littermates ($Bcl6^{+/-}$; Fig. 2, A and B). Consistently, histomorphometric analysis of $Bcl6^{-/-}$ mice demonstrated increased osteoclastogenesis and large osteoclast formation in $Bcl6^{-/-}$ mice. $Bcl6^{-/-}$ mice also showed elevated levels of serum C-terminal telopeptides of type I collagen (CTx) and decreased bone parameters (Fig. 2, C and D, and Fig. S2). In vitro, osteoclast progenitor cells isolated from Bcl6-deficient mice and treated with RANKL differentiated more rapidly into multinuclear tartrate-resistant acid phosphatase (TRAP)–positive cells than did those from control mice (Fig. 2 E and not depicted). Lower concentrations of RANKL not sufficient to differentiate control cells induced osteoclast differentiation of Bcl6-deficient cells (Fig. 2 E). Furthermore, increased bone resorbing activity was evident in Bcl6-deficient osteoclasts (Fig. 2 F), suggesting loss of a negative regulator of osteoclast function and differentiation. Deletion of Bcl6 in osteoclast precursor cells did not alter cell proliferation or induce apoptosis (Fig. S3). Thus, Bcl6 functions to regulate osteoclast differentiation and bone homeostasis, and its down-regulation by RANKL is required for osteoclast formation.

Blimp1 regulates Bcl6 expression and osteoclastogenesis
Next, we searched for a factor that might suppress Bcl6 during osteoclastogenesis and found that the transcriptional
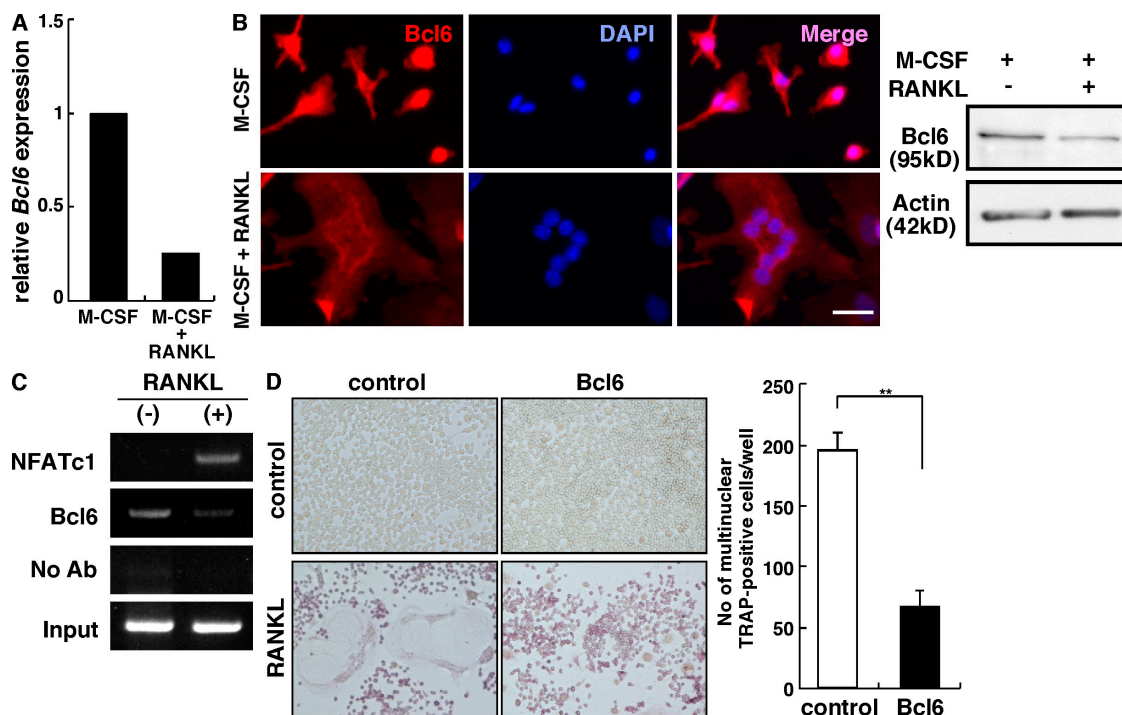
Figure 1. Bcl6 is suppressed during osteoclastogenesis and inhibits osteoclast formation. (A) *Bcl6* expression was examined by comparative microarray analysis between osteoclast precursors (M-CSF) and osteoclasts (M-CSF + RANKL) cultured for 6 d. (B) BMMs were cultured with or without RANKL for 8 d and subjected to immunofluorescence staining (left) and immunoblot (right) for Bcl6. Nuclei were visualized by DAPI. Bar, 25 μm. (C) Recruitment of NFATc1 and Bcl6 to the *NFATc1* P1 distal promoter was detected by ChIP assay. RAW264.7 cells were stimulated with or without RANKL for 48 h and subjected to ChIP analysis. (D) RAW264.7 cells transduced with Bcl6-overexpressing (Bcl6) or mock (control) retrovirus were cultured in the presence (RANKL) or absence (control) of RANKL for 5 d and stained with TRAP. Left, TRAP staining. (right) Numbers are means ± SD of multinuclear TRAP-positive cells in control or Bcl6-overexpressing RAW264.7 cells cultured with RANKL (**, P < 0.001; *n* = 6). Representative data of three independent experiments are shown (B–D).

repressor *Blimp1*, also called *Prdm1*, was specifically upregulated during osteoclast formation (Fig. S4 A). Blimp1 expression in osteoclasts was also demonstrated by using Blimp1-EGFP BAC transgenic mice, in which the EGFP sequence is knocked into the *Blimp1* locus, and by the observation that TRAP-positive cells showed Blimp1 expression (Fig. S4 B). RT-PCR analysis confirmed *Blimp1* induction in BMMs in the presence of RANKL in parallel with induction of *Ctsk*, a marker of osteoclast differentiation (Fig. 3 A). To determine whether Bcl6 is a Blimp1 target, an electrophoretic mobility shift assay (EMSA) was undertaken using a Bcl6 probe corresponding to a *Bcl6* regulatory region (Cimmino et al., 2008). Blimp1 formed a complex with the probe, but not with a Bcl6mut probe in which two nucleotides are changed to disrupt the Blimp1 binding sequence (Fig. S5 A). The PRDI probe, which corresponds to a region of the *interferon β* promoter known to bind Blimp1 protein (Keller and Maniatis, 1991) weakly but competitively, inhibited complex formation of the Bcl6 probe with Blimp1 (Fig. S5 A). In addition, unlabeled Bcl6 probe competed with labeled Bcl6 probe–Blimp1 to block complex formation, whereas unlabeled Bcl6mut probe did not (Fig. S5 A), confirming specificity and suggesting that Bcl6 is a direct Blimp1 target. Furthermore, ChIP analysis showed that, in the absence of

RANKL, Blimp1 was absent from the *Bcl6* promoter, but was recruited there by RANKL treatment (Fig. S5 B). Thus, we conclude that Bcl6 is a direct target of Blimp1 in osteoclasts.

To investigate physiological roles of Blimp1 in osteoclast differentiation, we established osteoclast-specific Blimp1 cKO mice ($Ctsk^{Cre/+}Blimp1^{flox/-}$), as Blimp1-null mice are embryonic lethal (Vincent et al., 2005). Blimp1 heterozygotes ($Blimp1^{+/-}$) were crossed with Ctsk-Cre mice ($Ctsk^{Cre/+}$) in which *Cre* is knocked into the *Ctsk* locus (Nakamura et al., 2007). Next, $Ctsk^{Cre/+}Blimp1^{+/-}$ mice were crossed with a transgenic strain harboring loxP-flanked (floxed) *Blimp1* alleles ($Blimp1^{flox/flox}$; Ohinata et al., 2005) to yield Blimp1 cKO mice. $Ctsk^{Cre/+}Blimp1^{flox/+}$ mice served as controls. Blimp1 cKO mice showed increased trabecular bone mass and an expanded growth plate compared with control mice, as seen by histomorphometric and microradiographical analysis (Fig. 3, B–D). TRAP staining of bone sections and analysis of serum CTx levels demonstrated severe inhibition of TRAP-positive osteoclast formation and bone resorbing activity, respectively (Fig. 3, E and F). Bone-morphometric analysis revealed reduced osteoblastic parameters in Blimp1 cKO mice (Fig. 3 C). Differentiation of osteoblasts isolated from osteoclast-specific Blimp1 cKO mice did not differ

from that seen in control mice (Fig. S6), suggesting that Blimp1 deficiency in osteoclast progenitor cells promotes decreased osteoblast differentiation and bone formation. Dele-

tion of Blimp1 in osteoclasts did not alter precursor cell proliferation or induction of apoptosis (Fig. S7, A and B). Furthermore, immune cell populations such as CD3-, B220-,
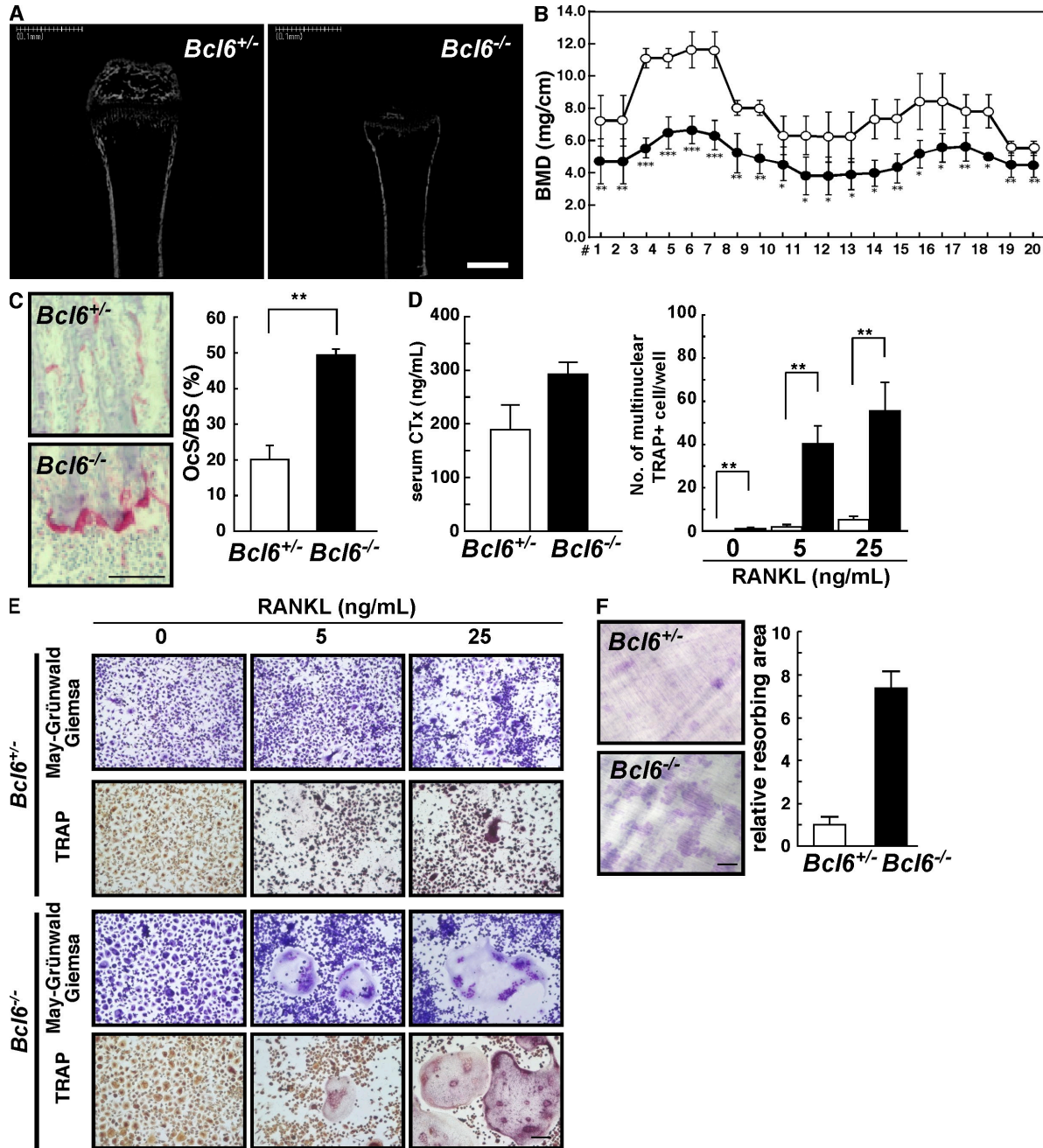

Figure 2. Increased osteoclast formation resulting from Bcl6 deficiency. (A) Micro focus CT analysis of femurs of *Bcl6+/−* (left) and *Bcl6−/−* (right) mice. (B) Bone mineral density (BMD) of equal longitudinal division of femurs of *Bcl6+/−* (open circles) and *Bcl6−/−* (closed circles) mice. Data are mean BMD (mg/cm²) ± SD (*, P < 0.05; **, P < 0.01; ***, P < 0.001; n = 3). (C) TRAP staining of tibial sections of *Bcl6+/−* (top) and *Bcl6−/−* (bottom) mice, and osteoclast surface as a percentage of bone surface (OcS/BS). Data are means ± SD (**, P < 0.001; n = 5). (D) Serum levels of C-terminal teropeptides of type I collagen (CTx) were analyzed in *Bcl6+/−* (white bar) and *Bcl6−/−* (shaded bar) mice. Data are means ± SD (**, P < 0.001; n = 3). (E) Osteoclast precursor cells from control (*Bcl6+/−*) or *Bcl6−/−* mice were cultured in the presence or absence of RANKL for 5 d and subjected to May-Grünwald Giemsa and TRAP staining, and the number of multinuclear TRAP-positive cells containing more than three nuclei was determined. Data are means ± SD of cells containing more than three nuclei (**, P < 0.001; n = 3). (F) Bone resorbing activity in *Bcl6+/−* (top) and *Bcl6−/−* (bottom) osteoclasts was analyzed by a pit formation assay. Representatives of at least three (E) and two (F) independent experiments are shown. Bars: (A) 1 mm; (C, E, and F) 100 μm.

Mac1-, or Gr1-positive cells were normal in the Blimp1 osteo-clast-specific KO, suggesting that Blimp1 is required to regulate osteoclast differentiation and bone homeostasis (Fig. S8).

Severe inhibition of osteoclastogenesis was also observed in in vitro culture. Multinuclear TRAP-positive osteoclast formation induced by RANKL was significantly inhibited in Blimp1 cKO cells (Fig. 4, A and B). *Blimp1* expression

was significantly up-regulated in the presence of RANKL in control cells; however, *Blimp1* induction was significantly inhibited in Blimp1 cKO cells (Fig. 4 C). In contrast, *Bcl6* expression was significantly down-regulated in control cells in the presence of RANKL; however, *Bcl6* expression in Blimp1 cKO cells was significantly up-regulated in Blimp1 cKO cells, even in the presence of RANKL (Fig. 4, C and D),
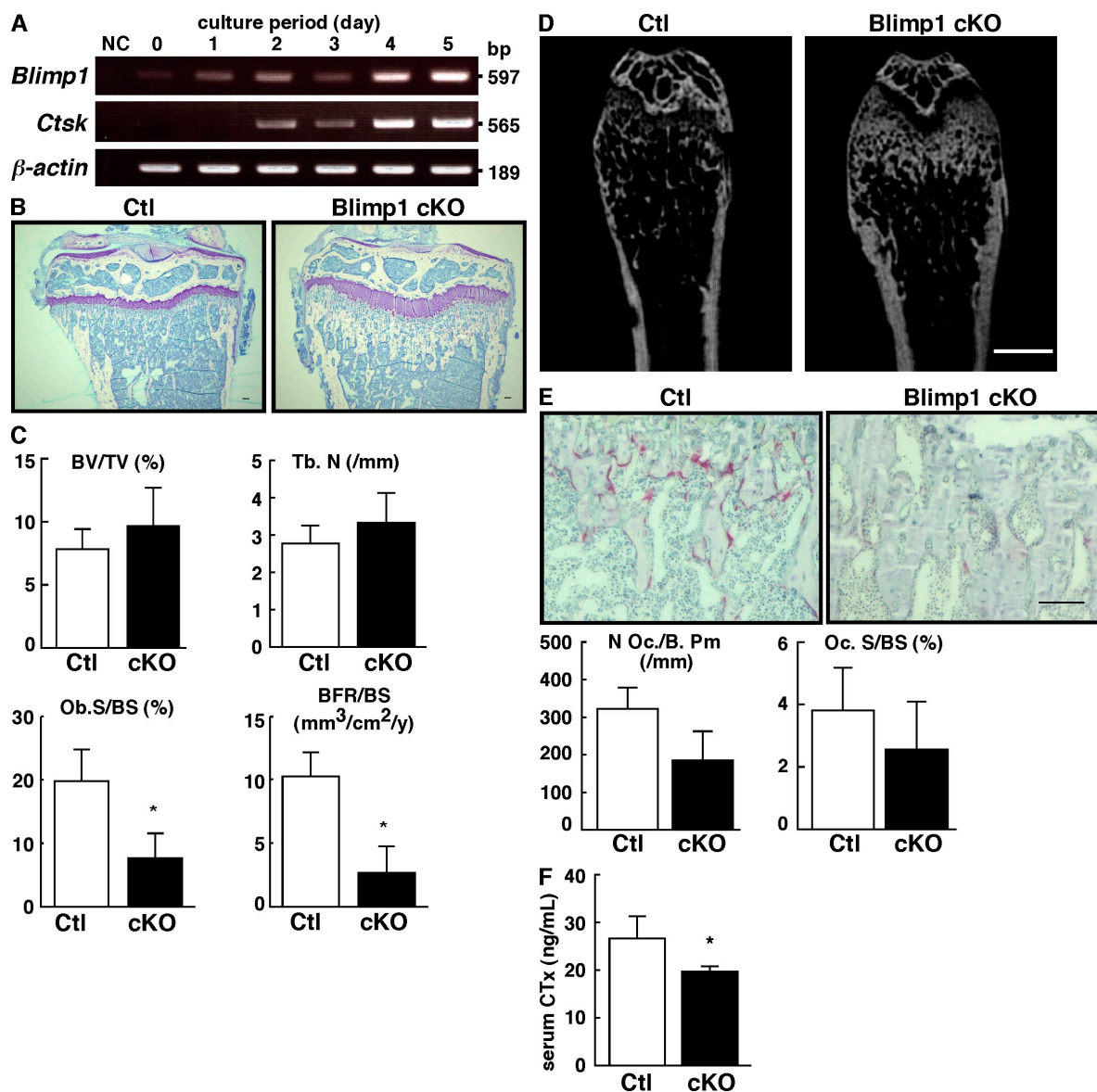
Figure 3. Blimp1 is essential for osteoclastogenesis and regulates bone homeostasis. (A) Total RNA isolated from BMMs cultured with M-CSF and RANKL for indicated periods was subjected to RT-PCR analysis with primers specific for *Blimp1* (top), *Ctsk* (middle), and β-actin (bottom). Representatives of at least three independent experiments are shown. (B–F) Bone phenotypes of osteoclast-specific Blimp1 KO (Blimp1 cKO) female mice at 8 wk old. (B) Longitudinal sections of tibias of control mice (Ctl; left) and Blimp1 cKO mice (right) were stained by toluidine blue. (C) Bone parameters are shown. Data are mean bone volume per total volume (BV/TV; %), trabecular number (Tb. N; /mm), osteoblast surface per bone surface (Ob.S/BS; %), or bone formation rate per bone surface (BFR/BS; mm^3/cm^2/y) ± SD of control (Ctl; white bar) and Blimp1 cKO (cKO; shaded bar) mice (*, P < 0.01; n = 5). (D) Microfocus CT analysis of femurs of control mice (Ctl; left) and Blimp1 cKO mice (right). (E) TRAP staining of tibial sections of control mice (Ctl; left) and Blimp1 cKO mice (right). Osteoclast parameters are shown as mean osteoclast number per bone perimeter (N.Oc/B.Pm) or osteoclast surface per bone surface (Oc.S/BS.) ± SD of control (Ctl; white bar) and Blimp1 cKO (cKO; shaded bar) mice (n = 5). (F) Serum CTx levels as a marker of bone resorption of control (Ctl; white bar) and Blimp1 cKO (cKO; shaded bar) mice (*, P < 0.01; n = 5). Bars: (B and E) 100 μm; (D) 1 mm.

suggesting that Blimp1 is critical to suppress *Bcl6* expression in osteoclasts during differentiation by RANKL and is essential for regulating osteoclastogenesis.

Bcl6 suppresses NFATc1 target genes during osteoclastogenesis

Expression of genes encoding osteoclastic factors, such as *NFATc1*, *DC-STAMP*, and *Ctsk*, all of which are targets of

NFATc1 (Matsumoto et al., 2004; Asagiri et al., 2005; Yagi et al., 2007), was markedly inhibited in Blimp1 cKO osteoclasts (Fig. 5 A). It was shown by ChIP analysis that NFATc1 was not evident on osteoclastic gene promoters without RANKL, but was recruited there after RANKL treatment of control cells (Fig. 5 B). In contrast, in the absence of RANKL, Bcl6 was present on osteoclastic gene promoters, but was lost from those promoters after RANKL treatment of control
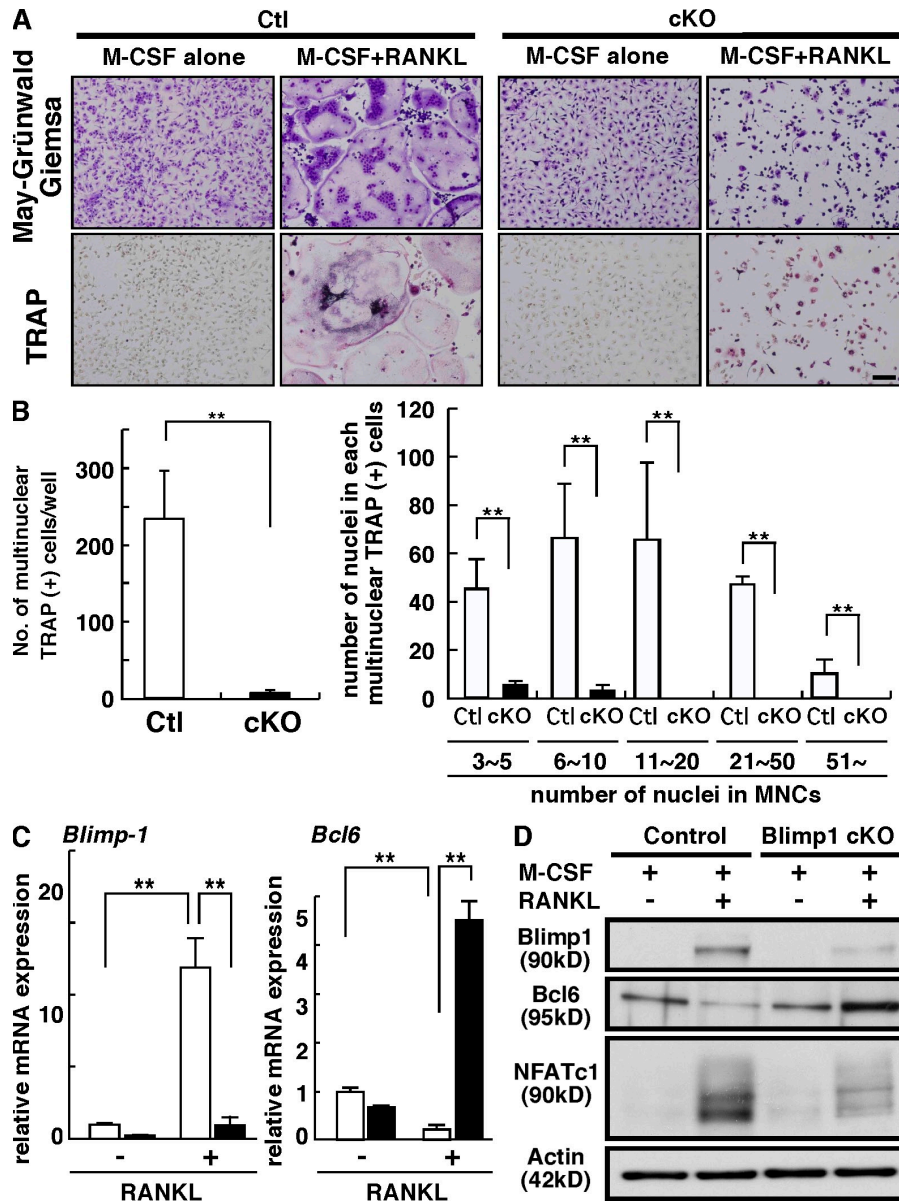

Figure 4.   Impaired osteoclastogenesis and Bcl6 expression resulting from Blimp1 deficiency. (A–C) BMMs from control (Ctl) or Blimp1 cKO (cKO) mice were cultured in the presence or absence of RANKL for 8 d. Cells were then subjected to May-Grünwald Giemsa and TRAP staining (A), the number of TRAP-positive cells containing more than three nuclei was scored (B, left), and the number of nuclei in each multinuclear osteoclast was determined (B, right). Bar, 100 µm. Numbers are means ± SD of multinuclear cells (**, P < 0.001; *n* = 3). (C) Total RNA was prepared from control (white bars) or Blimp1 cKO (shaded bars) cells treated with (+) or without (−) RANKL, and *Blimp1* (left) or *Bcl6* (right) expression relative to β-*actin* was analyzed by quantitative real-time PCR. Data represent means ± SD of *Blimp1*/β-*actin* or *Bcl6*/β-*actin* levels (**, P < 0.001; *n* = 4). (D) Whole-cell lysates from control or Blimp1 cKO cells cultured with M-CSF alone or M-CSF plus RANKL were analyzed by immunoblotting to detect Blimp1, Bcl6, and NFATc1. Actin was analyzed as an internal control. Representatives of at least four independent experiments are shown.

cells (Fig. 5 B). These data strongly indicate that NFATc1 and Bcl6 are reciprocally recruited to osteoclastic gene promoters. Significantly, reciprocal recruitment of NFATc1 and Bcl6 was severely impaired in Blimp1 cKO cells (Fig. 5 B), suggesting that Blimp1 up-regulation is critical for loss of Bcl6 from osteoclastic promoters after RANKL stimulation. Bcl6 was not present on the *NFATc2* promoter, which is not activated by RANKL stimulation (Asagiri et al., 2005), in the presence or absence of RANKL (Fig. 5 B), suggesting that Bcl6 is selectively recruited to promoters of osteoclastic genes and inhibits osteoclast differentiation. Whereas Bcl6 was down-regulated by RANKL treatment in control cells, Bcl6 expression was maintained in Blimp1 cKO cells, even in the presence of RANKL (Fig. 4 C and Fig. S9). These data indicate that impaired Bcl6 down-regulation caused by loss of Blimp1 results in continuous inhibition of osteoclastic gene expression, which in turn promotes severe inhibition of osteoclastogenesis and increased bone mass.

Finally, to confirm the role of Blimp1 in regulating osteoclastogenesis through Bcl6, osteoclast-specific Blimp1/Bcl6 double KO mice (double KO [DKO]; $Ctsk^{Cre/+}Blimp1^{flox/-}$ $Bcl6^{-/-}$ mice) were established (Fig. 6). DKO mice exhibited decreased bone mass in vivo compared with Blimp1 cKO mice (Fig. 6 A). Similarly, progenitor cells isolated from

DKO mice showed accelerated osteoclastogenesis compared with those from Blimp1 cKO mice (Fig. 6, B and C), suggesting that Blimp1 regulates osteoclastogenesis in part through controlling Bcl6. These results reveal that the Blimp1–Bcl6–osteoclastic molecule axis is critical for controlling osteoclast differentiation and bone homeostasis (Fig. 7).

DISCUSSION

Here, we show that two transcriptional repressors, Bcl6 and Blimp1, are essential to control physiological osteoclast development and maintenance of bone homeostasis. Bcl6, a member of the POZ/BTB-zinc finger protein family, suppresses expression of "osteoclastic" genes, all of which are targets of NFATc1 (Matsumoto et al., 2004; Asagiri et al., 2005; Yagi et al., 2007), thereby antagonizing NFATc1 function. Indeed, NFATc1 deficiency in osteoclasts results in impaired differentiation (Asagiri et al., 2005), whereas Bcl6-deficient mice exhibit accelerated osteoclast formation and decreased bone mass. Blimp1, encoded by *Prdm1*, acts as a suppressor of Bcl6, likely by direct binding to the *Bcl6* promoter. In contrast to Bcl6-deficient mice, osteoclast-specific Blimp1 cKO mice display impaired osteoclast differentiation and increased bone mass. Expression of *Bcl6* and *Blimp1* is reciprocal in normal osteoclast formation, and unusual elevation
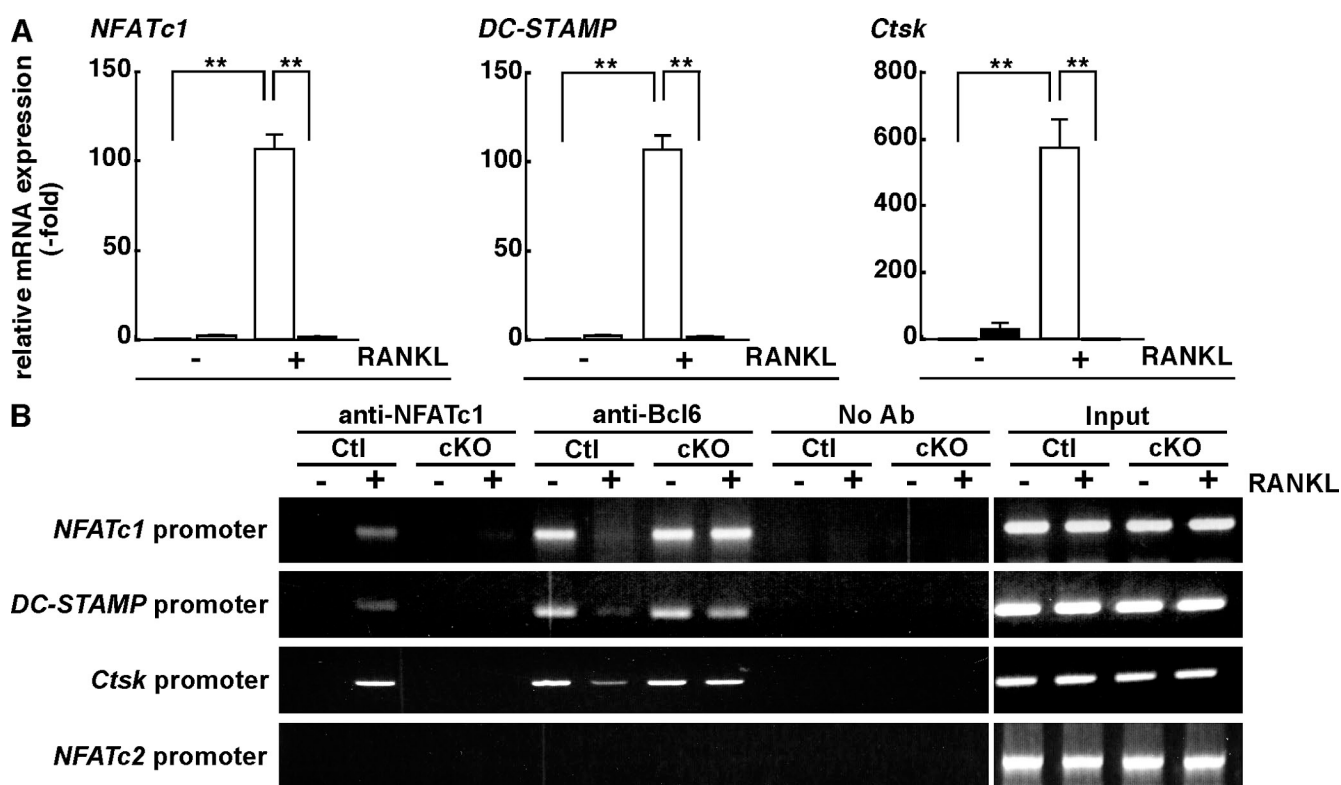

Figure 5. Bcl6 suppresses osteoclast differentiation. (A) Total RNA was prepared from control (white bars) or Blimp1 cKO (shaded bars) cells treated with (+) or without (−) RANKL, and the expression of the osteoclastic genes *NFATc1*, *DC-STAMP*, and *Ctsk* relative to β-actin was analyzed by a quantitative real-time PCR. Data are means ± SD of *osteoclastic genes/β-actin*. (**, P < 0.001; *n* = 4). (B) Recruitment of NFATc1 and Bcl6 to promoters of osteoclastic genes such as *NFATc1*, *DC-STAMP*, *Ctsk*, or a negative control gene *NFATc2* was analyzed by a ChIP assay. Representatives of at least four (A) or two (B) independent experiments are shown.
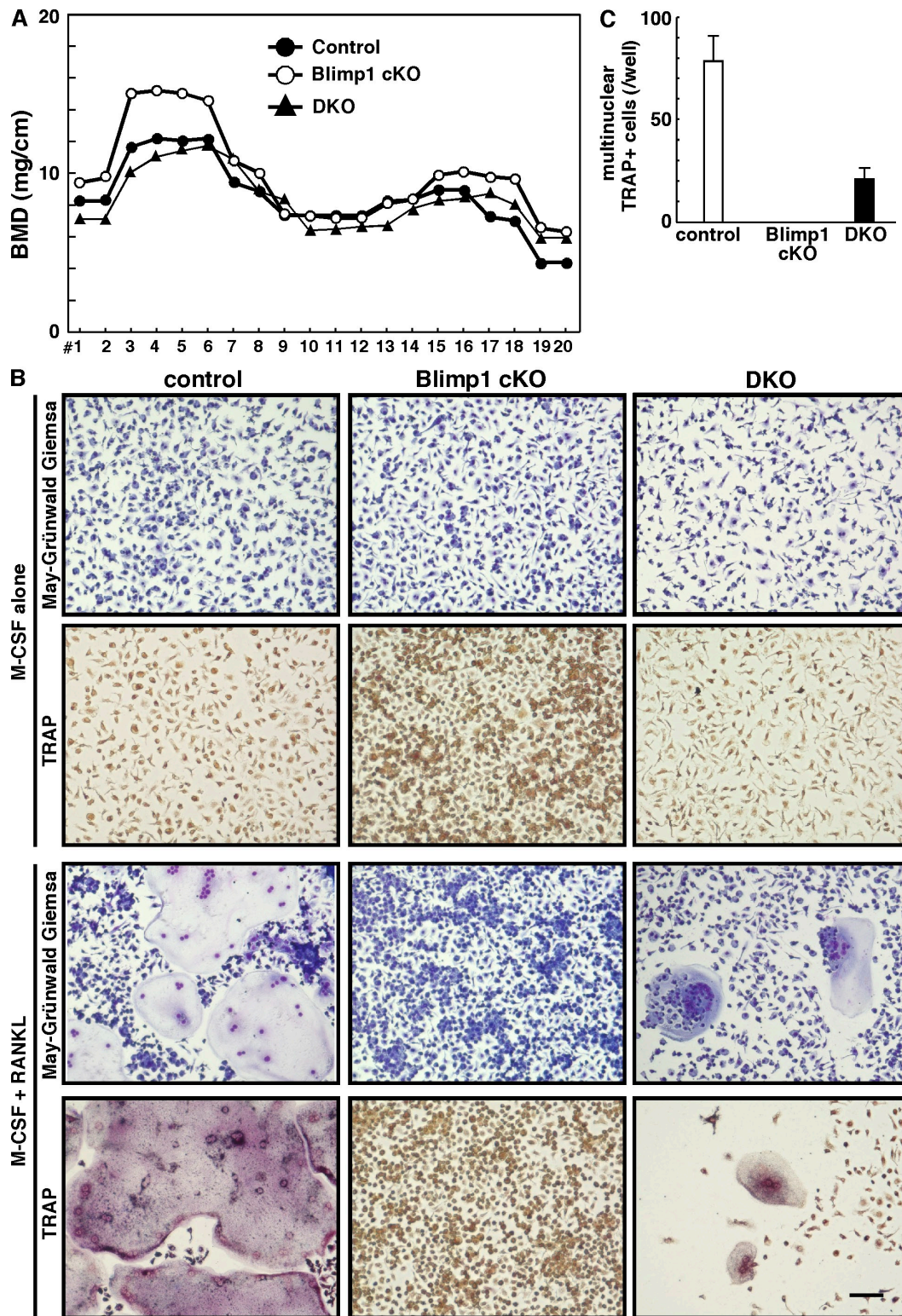
Figure 6. Bcl6 is a target of Blimp1 during osteoclastogenesis. (A) Bone mineral density (BMD) of equal longitudinal division of femurs of control (filled circles), Blimp1 cKO (open circles), and Blimp1 cKO/Bcl6 KO (DKO; filled triangles) mice. Data represent mean BMD ($n = 4$). (B and C) Osteoclast progenitor cells from control, Blimp1 cKO or DKO mice were cultured in the presence of M-CSF alone or M-CSF plus RANKL for 8 d. Cells were then subjected to May-Grünwald Giemsa and TRAP staining (B), and the number of TRAP-positive cells containing more than three nuclei was scored (C). Results are representative of three independent experiments. Bar, 100 µm.

of *Bcl6* expression caused by Blimp1 deficiency leads to osteoclastogenesis failure, as indicated by increased bone mass seen in a Blimp1 cKO model. Signals positively regulating NFATc1 in osteoclasts, such as TRAF6, c-Fos, ITAM-PLCγ-Ca^{2+} signals, Btk, and Tec (Takayanagi et al., 2002; Koga et al., 2004; Shinohara et al., 2008), have been characterized, and NFATc1 reportedly positively autoregulates in osteoclasts (Asagiri et al., 2005). However, factors modulating this activity have not been described. Our study characterizes such an axis of factors that serve as a molecular switch to control osteoclastogenesis and bone homeostasis after RANKL stimulation.

To date, the skeletal and immune systems have been shown to share common molecules to achieve homeostasis (Nakashima and Takayanagi, 2008). RANKL and RANK were originally identified in T cells and DCs (Anderson et al., 1997), respectively, and both are essential for osteoclastogenesis (Kong et al., 1999; Dougall et al., 1999). NFATc1 was identified in T cells and plays an essential role in osteoclast formation (Northrop et al., 1994; Asagiri et al., 2005). DC-STAMP plays a role in DC function and is required for cell–cell fusion of osteoclasts and macrophage giant cells (Yagi et al., 2005, 2007; Sawatani et al., 2008). Besides roles in immune system, Bcl6 has antiapoptotic and protooncogenic function
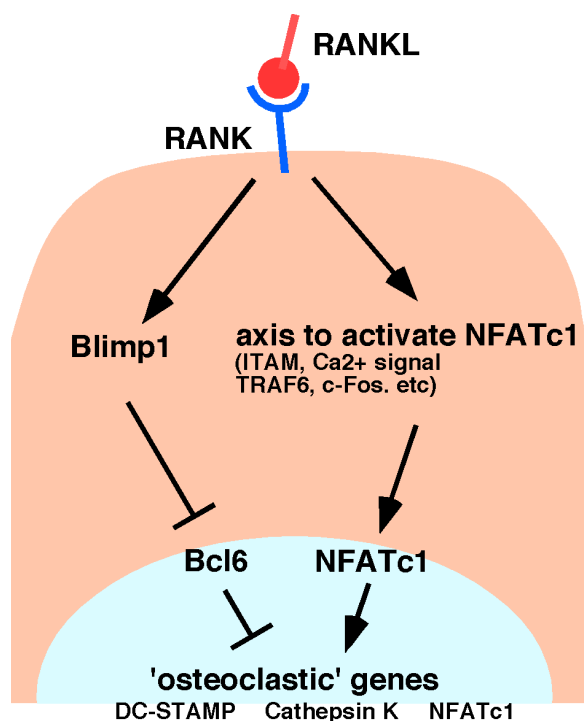

Figure 7. A schematic model of osteoclastogenesis regulated by the Blimp1–Bcl6–osteoclastic gene axis. RANKL–RANK interaction results in Blimp1 induction, leading to Bcl6 down-regulation and dissociation of Bcl6 from osteoclastic gene promoters, an event critical for osteoclastogenesis. NFATc1 activation is induced by various factors, such as ITAM, TRAF6, c-Fos, and Ca^{2+} signaling, which are also activated by RANKL.

(Baron et al., 2002; Ohno, 2006). Blimp1 also functions in specification of the germ cell lineage and acts as a tumor suppressor (Ohinata et al., 2005; John and Garrett-Sinha, 2009). Here, we show that Bcl6 and Blimp1, which are both implicated in B cell and T cell development (Turner et al., 1994; Fukuda et al., 1997; Dent et al., 1998; Kusam et al., 2003; Ichii et al., 2004; Kallies et al., 2006; Martins et al., 2006; Cimmino et al., 2008), have a novel function in regulating osteoclastogenesis and maintenance of bone homeostasis. It has been reported that Blimp1 represses Bcl6 (Cimmino et al., 2008) or that Blimp1 and Bcl6 regulate each other (Shapiro-Shelef and Calame, 2005). Blimp1 expression was reportedly inhibited by Bcl6 (Martins et al., 2006); however, we did not detect dysregulation of Blimp1 expression in Bcl6-deficient osteoclasts (unpublished data). Osteoclast-specific Blimp1/Bcl6 DKO mice exhibited increased osteoclastogenesis with decreased bone mass compared with Blimp1 cKO mice, indicating that Blimp1 regulates Bcl6 in osteoclasts. However, although Bcl6-deficient cells showed accelerated osteoclastogenesis compared with control cells, DKO cells showed decreased osteoclast differentiation compared with control cells, suggesting that Blimp1 regulates osteoclastogenesis through Bcl6 along with other target molecules. Blimp1 has multiple targets in lymphocytes and PGCs (Shaffer et al., 2002; Kurimoto et al., 2008), and thus it is possible that Blimp1 has multiple targets in osteoclasts as well. In osteoclasts, several negative regulators for osteoclastogenesis, such as *Id*, *Mafb*, and *Irf*8, have been identified (Lee et al., 2006; Kim et al., 2007; Zhao et al., 2009). Blimp1 may also target these molecules in osteoclasts to stimulate osteoclast differentiation. Further investigations are needed to clarify the molecular mechanisms of the regulation of osteoclastogenesis by Blimp1.

We used *Ctsk*$^{Cre/+}$ mice to establish osteoclast-specific Blimp1 cKO mice because *Ctsk*$^{Cre/+}$ mice have been used to generate osteoclast-specific KOs of factors such as the estrogen receptor and Bcl-XL (Nakamura et al., 2007; Iwasawa et al., 2009). Osteoclastogenesis, including *Ctsk* expression, has been evaluated in osteoclast-specific gene-targeted cells (Nakamura et al., 2007). *Blimp1* expression is induced earlier than *Ctsk* (Fig. 3 A), and osteoclastogenesis is inhibited in Blimp1 cKO cells, suggesting that continuous Blimp1 expression is required for full osteoclast differentiation under control of RANKL. Blimp1 is also known to be induced by BMP4 and LIF in PGCs, where it functions as a transcriptional repressor (Ohinata et al., 2009). In osteoclasts, Blimp1 is induced by RANKL and acts to repress Bcl6. Thus, signaling regulating Blimp1 expression differs between PGCs and osteoclasts.

Bone homeostasis requires a delicate balance between osteoclastic and osteoblastic activities. A decline in bone volume is closely related to up-regulation of osteoclast activity, and thus osteoclasts could be targeted therapeutically to treat skeletal disorders such as osteoporosis and destructive bone metastasis. FK506, a specific inhibitor of calcineurin–NFATs, inhibits osteoclastogenesis, but does not increase bone mass, as FK506 also inhibits bone formation (Koga et al., 2005). Thus, additional factors that could negatively regulate osteoclast

differentiation, such as those identified here, have been sought. Thus, our study provides new insight into regulation of osteoclastogenesis and bone homeostasis and forms the basis for developing novel therapeutic approaches to treat skeletal disorders.

MATERIALS AND METHODS

Mice. *Bcl6*$^{-/-}$ mice on a mixed C57BL/6 X 129/Sv background were generated by crossing *Bcl6* heterozygotes (*Bcl6*$^{+/-}$; Fukuda et al., 1997). Osteoclast-specific Blimp1 cKO mice on a C57BL/6 background were generated from three lines: mice carrying *loxP*-flanked *Blimp1* alleles (*Blimp1*$^{flox/flox}$; Ohinata et al., 2005), mice harboring *Cre* in the *Ctsk* (*Ctsk*$^{Cre/-}$) locus (Nakamura et al., 2007), and *Blimp1* heterozygotes (*Blimp1*$^{+/-}$; provided by A. Tarakhovsky, The Rockefeller University, New York, NY). Animals were maintained under specific pathogen–free conditions in animal facilities certified by the Keio University School of Medicine animal care committee. Animal protocols were approved by the Keio University School of Medicine animal care committee.

In vitro osteoclast formation. BM cells isolated from long bones (femurs, tibias, and humerus) were cultured 72 h in αMEM (Sigma-Aldrich) containing 10% heat-inactivated FBS (JRH Biosciences) and GlutaMax supplemented with M-CSF (50 ng/ml; Kyowa Hakko Kirin Co.). Adherent cells were then collected for analysis. 10^5 cells were cultured with M-CSF and recombinant soluble RANKL (25 ng/ml; PeproTech Ltd.) for indicated time periods. Mouse spleen cells were cultured overnight in αMEM containing 10% heat-inactivated FBS and GlutaMax supplemented with M-CSF. After this incubation, nonadherent cells were collected and 10^5 cells were cultured with M-CSF and recombinant soluble RANKL (5 or 25 ng/ml) for the indicated time periods. Osteoclastogenesis was evaluated by TRAP and May-Grünwald Giemsa staining (Miyamoto et al., 2000; Yagi et al., 2005). RAW264.7 cells were maintained in αMEM containing 10% heat-inactivated FBS and GlutaMax and stimulated by recombinant soluble RANKL to induce osteoclast formation.

Pit formation assay. Bone resorbing activity of osteoclasts was analyzed as previously described (Iwamoto et al., 2004). In brief, osteoclast precursors isolated from indicated mice were seeded on dentin slices and cultured in the presence of M-CSF plus RANKL for 6 d. Dentin slices were then stained by toluidine blue and observed under a microscope (model BZ-9000; Keyence Co.).

Analysis of skeletal morphology. Bcl6$^{-/-}$, DKO, and control littermates were necropsied 16 d after birth. Hindlimbs were removed, fixed with 70% ethanol, and subjected to dual-energy x-ray absorptiometry analysis to measure bone mineral density and for bone-histomorphometric analysis. Female 8-wk-old Blimp1 cKO mice and control littermates were administered intraperitoneal injections of 16 mg/kg calcein (Dojindo Co.) at 6 and 1 d before sacrifice to evaluate bone formation rate. Hindlimbs were removed and analyzed as described above.

ELISA. Serum levels of osteocalcin and C-terminal telopeptides of type I collagen (CTx) were measured by the Mouse Osteocalcin EIA kit (Biomedical Technologies Inc.) and RatLaps EIA (Immunodiagnostics Systems Ltd.), respectively. Assays were undertaken following the manufacturers' instructions.

Real-time PCR analysis. Total RNAs were isolated from BM cultures by TRIzol reagent (Invitrogen). After denaturation of total RNAs at 70°C for 5 min, cDNAs were synthesized from total RNAs using oligo(dT) primer and reverse transcription (Wako Pure Chemicals Industries). Real-time PCR was performed using SYBR Premix ExTaq II (Takara Bio Inc.) with the DICE Thermal cycler (Takara Bio Inc.), according to the manufacturer's instructions. Samples were matched to a standard curve generated by amplifying

serially diluted products using the same PCR reactions. *β-actin* expression served as an internal control. Primer sequences were as follows: *β-actin* forward: 5′-TGAGAGGGAAATCGTGCGTGAC-3′; *β-actin* reverse: 5′-AAGAAGGAAGGCTGGAAAAGAG-3′; *Bcl6* forward: 5′-AGACGCACAGTGACAAACCATACAA-3′; *Bcl6* reverse: 5′-GCTCCACAAATGTTACAGCGATAGG-3′; *Blimp1* forward: 5′-TTCTTGTGTGGTATTGTCGGGACTT-3′; *Blimp1* reverse: 5′-TTGGGGACACTCTTTGGGTAGAGTT-3′; *Ctsk* forward: 5′-ACGGAGGCATTGACTCTGAAGATG-3′; *Ctsk* reverse: 5′-GGAAGCACCAACGAGAGGAGAAAT-3′; *DC-STAMP* forward: 5′-TCCTCCATGAACAAACAGTTCCAA-3′; *DC-STAMP* reverse: 5′-AGACGTGGTTTAGGAATGCAGCTC-3′; *NFATc1* forward: 5′-CAAGTCTCACCACAGGGCTCACTA-3′; *NFATc1* reverse: 5′-GCGTGAGAGGTTCATTCTCCAAGT-3′; *type I collagen* forward: 5′-CCTGGTAAAGATGGTGCC-3′; *type I collagen* reverse: 5′-CACCAGGTTCACCTTTCGCACC-3′; *osteocalcin* forward: 5′-TAGCAGACACCATGAGGACCCT-3′; *osteocalcin* reverse: 5′-TGGACATGAAGGCTTTGTCAGA-3′.

Immunofluoresence. Cells were fixed with 4% paraformaldehyde (Wako Pure Chemical Industries) in PBS solution for 15 min at room temperature. After washing to remove fixation solution, cells were permeabilized in PBS containing 0.1% Triton X-100 for 10 min at room temperature and then washed. Nonspecific antibody binding was blocked by treatment with 5% BSA (Sigma-Aldrich Co.) in PBS. Cells were then stained with anti-Bcl6 antibody (1:50 dilution, N-3; Santa Cruz Biotechnology, Inc.) at 4°C overnight, washed with PBS and stained with Alexa Fluor 546–conjugated anti-rabbit IgG antibody (1:200 dilution) for 1 h at room temperature. Cells were washed to remove secondary antibody and incubated with DAPI solution (Dojindo Co.; 1:5,000) for nuclear staining, followed by microscopic observation (model BZ-9000; Keyence Co).

Immunoblotting analysis. Whole-cell lysates were prepared from BM cultures using RIPA buffer (1% Triton X-100, 1% sodium deoxycholate, 0.1% SDS, 150 mM NaCl, 10 mM Tris-HCl, pH 7.5, 5 mM EDTA, and a protease inhibitor cocktail; Sigma-Aldrich). Equivalent amounts of protein were separated by SDS-PAGE and transferred to a PVDF membrane (Millipore). Proteins were detected using the following antibodies: anti-NFATc1 (7A6), anti-Blimp1 (6D3), anti-Bcl6 (N-3) (Santa Cruz Biotechnology, Inc.), and anti-actin (A2066; Sigma-Aldrich).

EMSA. Nuclear extracts were prepared from COS7 cells transfected with pCAG-HA-Blimp1 or pCAG. Each extract was incubated for 30 min on ice with a [^{32}P]labeled probe in binding buffer (10 mM Tris-HCl, pH 7.9, 50 mM NaCl, 0.5 mM EDTA, 1 mM DTT, and 10% glycerol) containing 2 µg of poly(dI-dC), KCl, and BSA. Complexes were separated on 5% polyacrylamide gels in TGE buffer (25 mM Tris-HCl, 190 mM glycine, and 1 mM EDTA). The Bcl6 probe corresponding to a putative Blimp1 binding site in the *Bcl6* gene was 5′-AGGTTTCATAGGAAGTGAAAACCCTGCTAT-3′. A mutated probe (underlined residues) served as a negative control (Bcl6mut probe; 5′-AGGTTTCATAGGAAGTTAGAACCCTGCTAT-3′). After electrophoresis, gels were dried and exposed to the imaging plate, and signals were analyzed using ImageGauge software on the BAS2000 image analyzer (Fuji Film Co.).

ChIP. ChIP was performed on osteoclasts. M-CSF–induced BMMs were cultured on 100-mm type I collagen-coated culture dishes (Asahi Glass Co.) with M-CSF and recombinant RANKL for the indicated time periods, and then subjected to ChIP analysis using the ChIP-IT Enzymatic kit (ActivMotif Inc.), according to the manufacturer's instructions. Immunoprecipitation was performed using anti-NFATc1 (7A6), anti-Bcl6 (N-3), and anti-Blimp1 (C14A4; Cell Signaling Technology). DNA was purified by QIAquick PCR purification kit (QIAGEN) and analyzed using primers corresponding to the following promoters: *NFATc1*-P1 promoter, 5′-CCGGGACGCCCATGCAATCTGTTAGTAATT-3′ (sense) and 5′-GCGGGTGCCCTGAGAAAGCTACTCTCCCTT-3′ (antisense); the *DC-STAMP* promoter, 5′-GGGGGTCCTCATTTCTACAACTCAT-3′

(sense) and 5′-GCCACATCACCCTGAATCAATCTT-3′ (antisense); the *Ctsk* promoter, 5′-CCTTAAACTGGCTCCTGTCAAAGA-3′ (sense) and 5′-CCCTTCTTCAGAAGCCCTGTAAT-3′ (antisense); *NFATc2* promoter, 5′-TTATCAGGGAGCACTGCCCATCTCCGCTTT-3′ (sense) and 5′-CGGTCTGGCCTGAGCGACAGGCCCAGACAA-3′ (antisense); and *Bcl6* promoter, 5′-CAGCCACCCTGAGTTTACAA-3′ (sense) and 5′-CGTTCCAGCACTGTTTTGAA-3′ (antisense).

Microarray analysis. BM cells were isolated from 8-wk-old mouse and cultured in the presence of M-CSF for 3 d. M-CSF–dependent adherent cells were harvested and cultured with M-CSF alone for macrophages and M-CSF plus RANKL for osteoclasts, respectively. After 6 days of cultivation, total RNA was isolated and microarray analysis was undertaken using GeneChip Mouse Genome 430 2.0 Array (Affymetrix). Data were analyzed using GeneChip Operating Software and deposited in Minimum Information about a Microarray Experiment compliant in Gene Expression Omnibus (GEO accession no. GSE20850).

Online supplemental material. Fig. S1 shows that *Bcl6* is transcriptionally repressed by RANKL. Fig. S2 shows bone parameters of *Bcl6*^{+/−} and *Bcl6*^{−/−} mice. Fig. S3 shows proliferation and apoptosis of osteoclast precursors from *Bcl6*^{+/−} and *Bcl6*^{−/−} mice. Fig. S4 shows Blimp1 expression in osteoclasts. Fig. S5 shows that Blimp1 binds to the Bcl6 promoter. Fig. S6 shows normal osteoblastic differentiation in Blimp1 cKO cells. Fig. S7 shows proliferation and apoptosis of osteoclast precursors from Blimp1 cKO and control mice. Fig. S8 shows immune cell populations in spleens of Blimp1 cKO and control mice. Fig. S9 shows dysregulation of Bcl6 in Blimp1 cKO BMM. Online supplemental material is available at http://www.jem.org/cgi/content/full/jem.20091957/DC1.

REFERENCES

Anderson, D.M., E. Maraskovsky, W.L. Billingsley, W.C. Dougall, M.E. Tometsko, E.R. Roux, M.C. Teepe, R.F. DuBose, D. Cosman, and L. Galibert. 1997. A homologue of the TNF receptor and its ligand enhance T-cell growth and dendritic-cell function. *Nature*. 390:175–179. doi:10.1038/36593

Asagiri, M., K. Sato, T. Usami, S. Ochi, H. Nishina, H. Yoshida, I. Morita, E.F. Wagner, T.W. Mak, E. Serfling, and H. Takayanagi. 2005. Autoamplification of NFATc1 expression determines its essential role in bone homeostasis. *J. Exp. Med*. 202:1261–1269. doi:10.1084/jem.20051150

Baron, B.W., J. Anastasi, M.J. Thirman, Y. Furukawa, S. Fears, D.C. Kim, F. Simone, M. Birkenbach, A. Montag, A. Sadhu, et al. 2002. The human programmed cell death-2 (PDCD2) gene is a target of BCL6 repression: implications for a role of BCL6 in the down-regulation of apoptosis. *Proc. Natl. Acad. Sci. USA*. 99:2860–2865. doi:10.1073/pnas.042702599

Cimmino, L., G.A. Martins, J. Liao, E. Magnusdottir, G. Grunig, R.K. Perez, and K.L. Calame. 2008. Blimp-1 attenuates Th1 differentiation by repression of ifng, tbx21, and bcl6 gene expression. *J. Immunol*. 181:2338–2347.

Dent, A.L., J. Hu-Li, W.E. Paul, and L.M. Staudt. 1998. T helper type 2 inflammatory disease in the absence of interleukin 4 and transcription factor STAT6. *Proc. Natl. Acad. Sci. USA*. 95:13823–13828. doi:10.1073/pnas.95.23.13823

Dougall, W.C., M. Glaccum, K. Charrier, K. Rohrbach, K. Brasel, T. De Smedt, E. Daro, J. Smith, M.E. Tometsko, C.R. Maliszewski, et al. 1999. RANK is essential for osteoclast and lymph node development. *Genes Dev*. 13:2412–2424. doi:10.1101/gad.13.18.2412

Fukuda, T., T. Yoshida, S. Okada, M. Hatano, T. Miki, K. Ishibashi, S. Okabe, H. Koseki, S. Hirosawa, M. Taniguchi, et al. 1997. Disruption of the Bcl6 gene results in an impaired germinal center formation. *J. Exp. Med*. 186:439–448. doi:10.1084/jem.186.3.439

Ichii, H., A. Sakamoto, Y. Kuroda, and T. Tokuhisa. 2004. Bcl6 acts as an amplifier for the generation and proliferative capacity of central memory CD8+ T cells. *J. Immunol*. 173:883–891.

Iwamoto, K., T. Miyamoto, N. Hosogane, I. Hamaguchi, M. Takami, K. Takagi, and T. Suda. 2004. Dimer formation of receptor activator of nuclear factor kappa B induces incomplete osteoclast formation. *Biochem. Biophys. Res. Commun*. 325:229–234. doi:10.1016/j.bbrc.2004.10.024

Iwasawa, M., T. Miyazaki, Y. Nagase, T. Akiyama, Y. Kadono, M. Nakamura, Y. Oshima, T. Yasui, T. Matsumoto, T. Nakamura, et al. 2009. The antiapoptotic protein Bcl-xL negatively regulates the bone-resorbing activity of osteoclasts in mice. *J. Clin. Invest*. 119:3149–3159.

John, S.A., and L.A. Garrett-Sinha. 2009. Blimp1: a conserved transcriptional repressor critical for differentiation of many tissues. *Exp. Cell Res*. 315:1077–1084. doi:10.1016/j.yexcr.2008.11.015

Kallies, A., E.D. Hawkins, G.T. Belz, D. Metcalf, M. Hommel, L.M. Corcoran, P.D. Hodgkin, and S.L. Nutt. 2006. Transcriptional repressor Blimp-1 is essential for T cell homeostasis and self-tolerance. *Nat. Immunol*. 7:466–474. doi:10.1038/ni1321

Karsenty, G., and E.F. Wagner. 2002. Reaching a genetic and molecular understanding of skeletal development. *Dev. Cell*. 2:389–406. doi:10.1016/S1534-5807(02)00157-0

Keller, A.D., and T. Maniatis. 1991. Identification and characterization of a novel repressor of beta-interferon gene expression. *Genes Dev*. 5:868–879. doi:10.1101/gad.5.5.868

Kim, K., J.H. Kim, J. Lee, H.M. Jin, H. Kook, K.K. Kim, S.Y. Lee, and N. Kim. 2007. MafB negatively regulates RANKL-mediated osteoclast differentiation. *Blood*. 109:3253–3259. doi:10.1182/blood-2006-09-048249

Koga, T., M. Inui, K. Inoue, S. Kim, A. Suematsu, E. Kobayashi, T. Iwata, H. Ohnishi, T. Matozaki, T. Kodama, et al. 2004. Costimulatory signals mediated by the ITAM motif cooperate with RANKL for bone homeostasis. *Nature*. 428:758–763. doi:10.1038/nature02444

Koga, T., Y. Matsui, M. Asagiri, T. Kodama, B. de Crombrugghe, K. Nakashima, and H. Takayanagi. 2005. NFAT and Osterix cooperatively regulate bone formation. *Nat. Med*. 11:880–885. doi:10.1038/nm1270

Kong, Y.Y., H. Yoshida, I. Sarosi, H.L. Tan, E. Timms, C. Capparelli, S. Morony, A.J. Oliveira-dos-Santos, G. Van, A. Itie, et al. 1999. OPGL is a key regulator of osteoclastogenesis, lymphocyte development and lymph-node organogenesis. *Nature*. 397:315–323. doi:10.1038/16852

Kurimoto, K., Y. Yabuta, Y. Ohinata, M. Shigeta, K. Yamanaka, and M. Saitou. 2008. Complex genome-wide transcription dynamics orchestrated by Blimp1 for the specification of the germ cell lineage in mice. *Genes Dev*. 22:1617–1635. doi:10.1101/gad.1649908

Kusam, S., L.M. Toney, H. Sato, and A.L. Dent. 2003. Inhibition of Th2 differentiation and GATA-3 expression by BCL-6. *J. Immunol*. 170:2435–2441.

Lee, J., K. Kim, J.H. Kim, H.M. Jin, H.K. Choi, S.H. Lee, H. Kook, K.K. Kim, Y. Yokota, S.Y. Lee, et al. 2006. Id helix-loop-helix proteins negatively regulate TRANCE-mediated osteoclast differentiation. *Blood*. 107:2686–2693. doi:10.1182/blood-2005-07-2798

Li, C.Y., K.J. Jepsen, R.J. Majeska, J. Zhang, R. Ni, B.D. Gelb, and M.B. Schaffler. 2006. Mice lacking cathepsin K maintain bone remodeling but develop bone fragility despite high bone mass. *J. Bone Miner. Res*. 21:865–875. doi:10.1359/jbmr.060313

Martins, G.A., L. Cimmino, M. Shapiro-Shelef, M. Szabolcs, A. Herron, E. Magnusdottir, and K. Calame. 2006. Transcriptional repressor Blimp-1 regulates T cell homeostasis and function. *Nat. Immunol*. 7:457–465. doi:10.1038/ni1320

Matsumoto, M., M. Kogawa, S. Wada, H. Takayanagi, M. Tsujimoto, S. Katayama, K. Hisatake, and Y. Nogi. 2004. Essential role of p38 mitogen-activated protein kinase in cathepsin K gene expression during

osteoclastogenesis through association of NFATc1 and PU.1. *J. Biol. Chem*. 279:45969–45979. doi:10.1074/jbc.M408795200

Miyamoto, T., F. Arai, O. Ohneda, K. Takagi, D.M. Anderson, and T. Suda. 2000. An adherent condition is required for formation of multinuclear osteoclasts in the presence of macrophage colony-stimulating factor and receptor activator of nuclear factor kappa B ligand. *Blood*. 96:4335–4343.

Nakamura, T., Y. Imai, T. Matsumoto, S. Sato, K. Takeuchi, K. Igarashi, Y. Harada, Y. Azuma, A. Krust, Y. Yamamoto, et al. 2007. Estrogen prevents bone loss via estrogen receptor alpha and induction of Fas ligand in osteoclasts. *Cell*. 130:811–823. doi:10.1016/j.cell.2007.07.025

Nakashima, T., and H. Takayanagi. 2008. The dynamic interplay between osteoclasts and the immune system. *Arch. Biochem. Biophys*. 473:166–171. doi:10.1016/j.abb.2008.04.004

Ng, D., N. Thakker, C.M. Corcoran, D. Donnai, R. Perveen, A. Schneider, D.W. Hadley, C. Tifft, L. Zhang, A.O. Wilkie, et al. 2004. Oculofaciocardiodental and Lenz microphthalmia syndromes result from distinct classes of mutations in BCOR. *Nat. Genet*. 36:411–416. doi:10.1038/ng1321

Northrop, J.P., S.N. Ho, L. Chen, D.J. Thomas, L.A. Timmerman, G.P. Nolan, A. Admon, and G.R. Crabtree. 1994. NF-AT components define a family of transcription factors targeted in T-cell activation. *Nature*. 369:497–502. doi:10.1038/369497a0

Ohinata, Y., B. Payer, D. O'Carroll, K. Ancelin, Y. Ono, M. Sano, S.C. Barton, T. Obukhanych, M. Nussenzweig, A. Tarakhovsky, et al. 2005. Blimp1 is a critical determinant of the germ cell lineage in mice. *Nature*. 436:207–213. doi:10.1038/nature03813

Ohinata, Y., H. Ohta, M. Shigeta, K. Yamanaka, T. Wakayama, and M. Saitou. 2009. A signaling principle for the specification of the germ cell lineage in mice. *Cell*. 137:571–584. doi:10.1016/j.cell.2009.03.014

Ohno, H. 2006. Pathogenetic and clinical implications of non-immunoglobulin; BCL6 translocations in B-cell non-Hodgkin's lymphoma. *J. Clin. Exp. Hematop*. 46:43–53. doi:10.3960/jslrt.46.43

Rodan, G.A., and T.J. Martin. 2000. Therapeutic approaches to bone diseases. *Science*. 289:1508–1514. doi:10.1126/science.289.5484.1508

Sato, K., A. Suematsu, T. Nakashima, S. Takemoto-Kimura, K. Aoki, Y. Morishita, H. Asahara, K. Ohya, A. Yamaguchi, T. Takai, et al. 2006. Regulation of osteoclast differentiation and function by the CaMK-CREB pathway. *Nat. Med*. 12:1410–1416. doi:10.1038/nm1515

Sawatani, Y., T. Miyamoto, S. Nagai, M. Maruya, J. Imai, K. Miyamoto, N. Fujita, K. Ninomiya, T. Suzuki, R. Iwasaki, et al. 2008. The role of DC-STAMP in maintenance of immune tolerance through regulation of dendritic cell function. *Int. Immunol*. 20:1259–1268. doi:10.1093/intimm/dxn082

Shaffer, A.L., K.I. Lin, T.C. Kuo, X. Yu, E.M. Hurt, A. Rosenwald, J.M. Giltnane, L. Yang, H. Zhao, K. Calame, and L.M. Staudt. 2002. Blimp-1 orchestrates plasma cell differentiation by extinguishing the mature B cell gene expression program. *Immunity*. 17:51–62. doi:10.1016/S1074-7613(02)00335-7

Shapiro-Shelef, M., and K. Calame. 2005. Regulation of plasma-cell development. *Nat. Rev. Immunol*. 5:230–242. doi:10.1038/nri1572

Shinohara, M., T. Koga, K. Okamoto, S. Sakaguchi, K. Arai, H. Yasuda, T. Takai, T. Kodama, T. Morio, R.S. Geha, et al. 2008. Tyrosine kinases Btk and Tec regulate osteoclast differentiation by linking RANK and ITAM signals. *Cell*. 132:794–806. doi:10.1016/j.cell.2007.12.037

Takayanagi, H., S. Kim, T. Koga, H. Nishina, M. Isshiki, H. Yoshida, A. Saiura, M. Isobe, T. Yokochi, J. Inoue, et al. 2002. Induction and activation of the transcription factor NFATc1 (NFAT2) integrate RANKL signaling in terminal differentiation of osteoclasts. *Dev. Cell*. 3:889–901. doi:10.1016/S1534-5807(02)00369-6

Turner, C.A. Jr., D.H. Mack, and M.M. Davis. 1994. Blimp-1, a novel zinc finger-containing protein that can drive the maturation of B lymphocytes into immunoglobulin-secreting cells. *Cell*. 77:297–306. doi:10.1016/0092-8674(94)90321-2

Vincent, S.D., N.R. Dunn, R. Sciammas, M. Shapiro-Shalef, M.M. Davis, K. Calame, E.K. Bikoff, and E.J. Robertson. 2005. The zinc finger transcriptional repressor Blimp1/Prdm1 is dispensable for early axis formation but is required for specification of primordial germ cells in the mouse. *Development*. 132:1315–1325. doi:10.1242/dev.01711

Yagi, M., T. Miyamoto, Y. Sawatani, K. Iwamoto, N. Hosogane, N. Fujita, K. Morita, K. Ninomiya, T. Suzuki, K. Miyamoto, et al. 2005. DC-STAMP is essential for cell-cell fusion in osteoclasts and foreign body giant cells. *J. Exp. Med*. 202:345–351. doi:10.1084/jem.20050645

Yagi, M., K. Ninomiya, N. Fujita, T. Suzuki, R. Iwasaki, K. Morita, N. Hosogane, K. Matsuo, Y. Toyama, T. Suda, and T. Miyamoto. 2007. Induction of DC-STAMP by alternative activation and downstream signaling mechanisms. *J. Bone Miner. Res*. 22:992–1001. doi:10.1359/jbmr.070401

Zhao, B., M. Takami, A. Yamada, X. Wang, T. Koga, X. Hu, T. Tamura, K. Ozato, Y. Choi, L.B. Ivashkiv, et al. 2009. Interferon regulatory factor-8 regulates bone metabolism by suppressing osteoclastogenesis. *Nat. Med*. 15:1066–1071. doi:10.1038/nm.2007